

Separation Modeling of Blood Cells using Dielectrophoretic Field Flow

Ayat Nada
Department of Computers and
Systems
Electronics Research Institute
Cairo, Egypt

Mohamed Omar
Biomedical Engineering
Department
Misr University for Science and
Technology
Giza, Egypt

Ahmed M. Sayed
Biomedical Engineering
Department
Helwan University
Cairo, Egypt

ABSTRACT

Improving the ability to separate particles and cells in a continuous flow pattern facilitates faster and incessant medical diagnosis. In this paper, a modified design is presented that is capable of separating platelet cells from other blood cells in a continuous flow. The modified device achieves the separation of platelets using Dielectrophoretics (DEP) mechanism. A two dimensional finite element model was exploited to test different design parameters, including the applied separation peak to peak voltage, frequency, and speed of the flow inlet. Simulations of the modified microfluidic device showed successful separation of the red blood cells from platelets and also from other mixed blood cells. The modeling and simulation results demonstrate that cell separation can be achieved with high purity levels of platelets of up to 99.8%. The device's optimized technology makes it suitable for portable, bedside and point-of-care testing applications.

Keywords

Microfluidics; Dielectrophoretics; Finite Element Model; Blood cell Separation; Platelets(PLTs).

1. INTRODUCTION

Platelets (PLTs) are one type of blood cells; they have a major function in the hemostasis process. Disturbances can be caused by the abnormal concentration of the platelets. The low concentration of platelets can cause bleeding, while the high level of platelets may lead to thrombosis and complications such as myocardial infarction, embolism or stroke [1]. Consequently necessary to screen the concentration level of platelets the early diagnosis of such changes enough to the proper treatment.

Now, various techniques have been utilized for separation, mainly between platelets (PLTs) and red blood cells (RBCs), including centrifugation [2], mechanical filtering [3], and antibody recognition [4]. Although, these techniques are macro-scale techniques, and have the following disadvantage: (1) The process of non-continuous separation which takes more time for analysis, (2) The requirements of a large size and adjust the samples, and (3) the requirement for very prepared staff to work the enormous and expensive tools [5] - [9]. Each of these technologies must face challenges relating to the size of the Cell (PLTs: 2–3 μm and RBCs: 7–8 μm), the comparatively low concentration of platelets compared with RBCs (2×10^8 PLTs/ml versus 5×10^9 RBCs/ml) and possible activation and coagulation of the platelets during handling.

Traditionally, micro-scale cell separation techniques take advantage of the variation in the intrinsic characteristics of the population of the different cell to accomplish separation. Mechanical and physical properties, including size, shape, density, adhesion, and deformability, are common markers for differentiation. Due to their high sensitivity and efficiency, the

separation of the cell by polarization and magnetic properties have become extremely popular in the recent years [10].

Recently, various separation techniques have been successfully applied to separate stem cells depend on their fundamental properties to conduct basic studies [10]–[12]. With advances in the technologies of microfluidic and analytical devices integrated on a mini chip-scale platform have become a promising alternative for diagnostic testing near the site of a patient, or point-of-care (POC) [13]–[17]. Microfluidics presents a functional toolset for cell separation have many advantages including, (i) low sample quantities and costly reagent volumes; (ii) quick test preparation, limiting examination time; (iii) high sensitivity and spatial resolution, increasing detection accuracy; (iv) integrated reference systems with little human intervention, reducing odds of sample contamination; (v) increased portability—potential for POC diagnostic in weakness of resources lacking clinical laboratories and skilled personnel; and (vi) cost reduction[18]–[20].

Finite element modeling (FEM) has become a vital tool in modern prototyping and testing [21–24]. Our finite element model aims to test the separation efficiency of platelets and red blood cells from blood micro-channels in the composition of H-filter and dielectrophoresis (DEP) combining low-voltage, a single-phase system to obtain dielectrophoresis field flow fractionation (DEP-FFF). Niccolo` Piacentini et al. [25] presented separation of cells through the changes in the characteristics of the dielectric, for example, live yeast cells and dead by dielectrophoretic. The rate among the values of the Clausius-Mossotti factor at the two different frequencies this parameter of cells called "opacity" used in sorting technology. However, the adoption of dielectrophoretic force on the size of the cell makes sorting the cells with major differences in size in the system based on opacity defy. Dielectrophoresis field flows fractionation lets to overcome this constraint. Cells separate relying on its size and lower voltages have been applied in this paper compared with the previous device designs.

The Proposed system able to separate platelets from blood utilizing a single-phase and low-voltage system adding micro-channels in the composition of the H-filter and achieve (DEP-FFF).

The paper is organized as follows: Section II presents the methods; design and modeling of the device. Section III presents the results. The discussion is presented in section IV. Finally; the conclusion is shown in Section V.

2. MATERIALS AND METHODS

2.1 Dielectrophoresis

Dielectrophoretics (DEP) is a phenomenon where applied force on dielectric particles when exposed to a non-uniform electric field. DC-DEP, applied a spatial non-uniform DC electric field on the induced movement of dielectric particles depended on the size characteristics will separate biological cells [26]. The separation force in electrical field E which an inhomogeneous and time-varying is proportional to the cell volume, as illustrated by equation (1) [27]. Thus, cells that have dielectric characteristics different will experience differential DEP forces when subjected to an inhomogeneous dc electric field [28].

$$F_{DEP}(t) = \sum_{k=0}^n 2\pi\epsilon_m r^3 Re(K_{CM}) \nabla |E_{RMS}|^2 \quad (1)$$

where ϵ_m is the permittivity of the medium, r the radius of the particle, $Re(K_{CM})$ is the real part of the Clausius-Mossotti factor, which is defined as:

$$K_{CM} = \frac{\epsilon_p - \epsilon_m}{\epsilon_p + 2\epsilon_m} \quad (2)$$

where ϵ_p and ϵ_m are the complex permittivities of the particle and suspending medium, respectively. Apparently, the KCM relied on the complex permittivities of the particle and suspending medium. Positive DEP (pDEP) created to attract the particle to the high electric field region when the suspending medium is less polarizable than particle (i.e., $Re(K_{CM}) > 0$). When the suspending medium is more polarizable than particle (i.e., $Re(K_{CM}) < 0$), negative DEP (nDEP) is created to repel the particle away from the highly electric field.

2.2 Geometry of the separation device

The present model is depended on a lab-on-a-chip device explained in detail in [25]. It consists of two inlets, two outlets and a separation region in which a non-uniform electric field generated by electrode arranged alternately change the particle paths. Blood mixture cells are injected at the entrance and buffer comes from two outlets. Because of the dimensions of the small path (40 μ m in width), the flow is laminar in the separation region (Reynolds number < 0.05), with the goal that is not confused by the two flows. Fig. 1 shows the schematic of the modeled geometry. As seen in the figure, the inlet flow speed for the lower inlet (853 μ m/s) is much higher than the upper inlet (134 μ m/s) to focus all the injected particles in the direction of the top outlet. When lower operating voltages are used in practicals, there is also a significant reduction in electrical heating and electro-chemical effects for a given desired DEP forces.

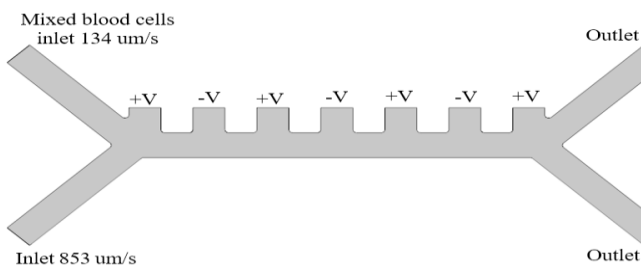


Fig. 1. The two-dimensional geometry of modeled device with inlets and outlets

2.3 Numerical Analysis

Numerical simulations were validated to evaluate each of convection, and dielectrophoretic forces (DEF) realistic on the cells. Software package COMSOL Multiphysics was used to perform the analysis of two-dimensional finite element model, where it returns distribution of electric field and the flow inside the geometry of device.

The model uses the following physical phenomena:

- (1) Crawl flow to demonstrate the fluid flow.
- (2) Trace particle-fluid flow to calculate the path of PLTs and RBCs under the effect of the force of dielectrophoretic and drag.
- (3) Electric currents to show the electric field in the device's microchannel.

The geometry of the device's channels and electrodes were defined in the graphics section of the COMSOL package. Sample and buffer inlets with channel widths of 40 μ m and height (200 μ m and -200 μ m) respectively, merge into the separation channel of 560 μ m width and 40 μ m length. The collection outlets have the same dimension of two inlets, followed by selecting appropriate materials for each domain and setting the electrical potential on the boundary of each electrode. Summary of the used parameters' values for RBCs and PLTs are listed in Table 1 [25, 27].

Table 1. Parameters used to calculate KCM of RBCs and PLTs

Cell	Membrane thickness (nm)	Diameter (μ m)	Relative permittivity, ϵ_r	Conductivity, σ (S/m)
RBCs	9	5	Membrane 44	10^{-6}
			Interior 59	0.31
PLTs	8	1.8	Membrane 6	10^{-6}
			Interior 50	0.25

Following that the meshing step was performed using a variety of element types, as listed in Table 2. The model meshing, as shown in Fig 2, was made using the default software's settings.

TABLE 2. Mesh Element statistics

Property	Value
Average element quality	0.8898
Triangular elements	7527
Quadrilateral elements	641
Edge elements	661
Vertex elements	59

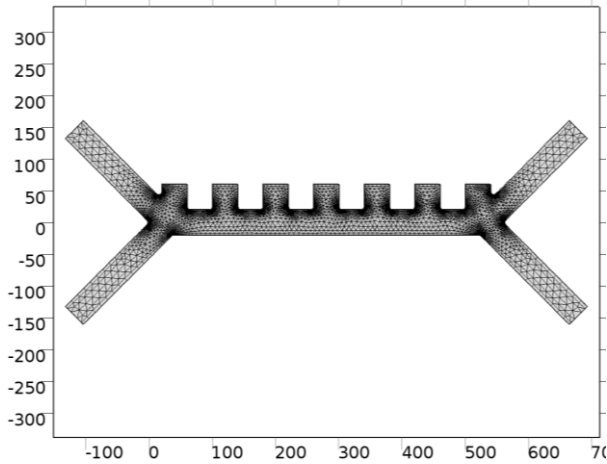


Fig. 2. The two-dimensional meshed model of the Dielectrophoretic separation device.

Given the beginning place somewhere in the cell entrance, follow the path of the cell through the recursive update the place subsequent the flow field and the DEP speed. Fig. 3 demonstrates the logical paths of the cells inside the device's geometry. This may be evidenced; it is conceivable to choose a blend of envelope focusing and nDEP where the PLT diverges enough to go to the left channel while the RBC remains on the right, because of the bifurcation moving as a laminar splitter.

The numerical verification of "stability" in sorting through analyzing the effect of the beginning place of the cells on the logical path. As will be shown in the simulation results, the device is able of keeping the performance of sort with changing place of the output by a small portion of the cell diameter, where the blood flow is highly focused on the left part of the channel.

3. RESULTS

Several steps were carried out to evaluate blood separation efficiency and red blood cell extraction volume when dielectrophoretic voltage is applied between adjacent liquid electrodes. Fig. 3 demonstrate a strong dissonance of the red blood cells away from the electrodes because of the existence of negative DEP (nDEP), making those large cells leave the separation region in the correct path. The effect on the left side displays the path of the platelets, which are too small to be clearly prevented and remain with the laminar flow on the left path and leave the separation region on the left path. The concentration level of red blood cells applied for this paper is lower than the concentration level of platelets to improve visualize the platelet path. The flow speed used at the upper inlet is $134 \mu\text{m/s}$ and the lower inlet is $853 \mu\text{m/s}$ to focus cells in the direction of the middle at the entrance because of the parabolic flow profile.

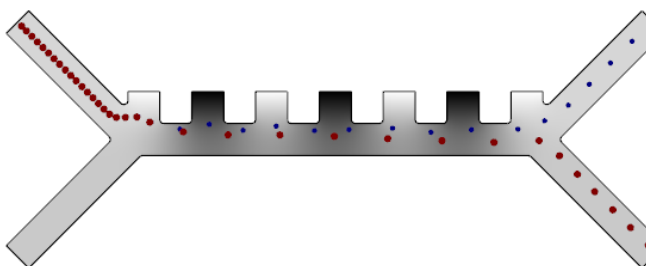


Fig. 3. Particle paths with dielectrophoretic force applied. The RBCs are displayed in red and the platelets in blue.

After flowing between the sorting electrodes, the cells are separated based on their different dielectric properties at specific frequencies. The frequency used for this initial model is 100 kHz where each of platelets and red blood cells is suffering negative DEP (nDEP). Nevertheless, the dielectrophoretic force is more tougher for the red blood cells than for the platelets because of the difference in size.

A first variation to the original system's design was performed, utilizing a voltage of 10Vpp, but at different frequencies ranging from 100kHz to 1MHz in incremental steps of 200kHz, as shown in Table III. The proposed device was able to separate platelets from other blood cells. Separation efficiency was found to be 98.8% at 100 kHz (the highest value that was reported in the literature [25]), and 97% at 1MHz. However, when the frequency was lowered than 100 kHz or frequency is increased from 10MHz to 1GHz the particles were not separated and followed as following a similar path, as shown in Fig.4.

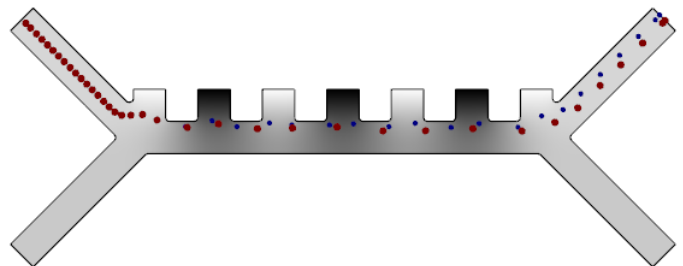


Fig. 4. The particles are released at the same time and follow a similar path (separation failure), for frequencies higher than 1MHz. RBCs are displayed in red and PLTs in blue.

Table 4. Frequency Change effect on Separation of Blood Cells

Amplitude	Inlets Flow Speed (Upper-Lower)	Frequency	Separation (Effeciancy)
10 V _{pp}	134 $\mu\text{m/s}$ -853 $\mu\text{m/s}$	<100kHz	Non- Separated
10 V _{pp}	134 $\mu\text{m/s}$ -853 $\mu\text{m/s}$	100kHz	Separated (effec: 98.8%)
10 V _{pp}	134 $\mu\text{m/s}$ -853 $\mu\text{m/s}$	>100 kHz to 1MHz	Separated (effec: 98.8% to 97%)
10 V _{pp}	134 $\mu\text{m/s}$ -853 $\mu\text{m/s}$	10MHz to 1GHz	Non- Separated

A second variation was performed on the device, using different electrode voltages at 100 kHz frequency; Table 5. The simulations showed that when applying voltages below 10 VPP and higher than 15 VPP the device was not able to separate platelets from other blood cells and followed a similar path, but it was capable of PLTs separation using 10 VPP and 15VPP only. It is worth mentioning that the separation efficiency at 20 VPP was not optimal and incomplete, so this was considered as a separation failure situation, as inconsistent results could be produced.

Table 5. Amplitude Change effect on Separation of Blood Cells

Amplitude	Inlets Flow Speed (Upper-Lower)	Frequency	Separation (Effeciency)
5 V _{PP}	134µm/s-853µm/s	100kHz	Non-Separated
15 V _{PP}	134µm/s-853µm/s	100kHz	Separated (99.6%)
20 V _{PP}	134µm/s-853µm/s	100kHz	Separated but not uniform (96.1%)
24 V _{PP}	134µm/s-853µm/s	100kHz	Non-Separated

A third variation to the original device’s design was performed to validate the operation of the device, using different flow speed velocities; Table V. Model simulations revealed that when applying inlet flow velocities from 134 to 500µm/s flow speed at upper inlet and 853 to 1200 µm/s at lower inlet the device was still able to separate platelets from other blood cells, but for lower inlet flow speed of 1500 µm/s and above, the particles were released at the same time and follow a similar path (separation failure). Applying a flow speed at the upper inlet with 134 to 300µm/s and increase flow speed lower inlet by 1300 µm/s, the proposed device was still capable of cell separation, but unable to separate platelets when flow speed was increased from 400 µm/s and above.

Table 6. Flow speed Change effect on Separation of Blood Cells

Amplitude	Inlets Flow Speed (Upper-Lower)	Frequency	Separation (Effeciency)
10V _{PP}	150 µm/s- 850 µm/s	100kHz	Separated (98.9%)
10V _{PP}	134µm/s-1300 µm/s	100kHz	Separated (97.3%)
10 V _{PP}	500µm/s-1200 µm/s	100kHz	Separated (96.3%)
10V _{PP}	400µm/s-1300 µm/s	100kHz	Non-Separated
10V _{PP}	500µm/s-1500µm/s	100kHz	Non-Separated
15 V _{PP}	150µm/s-850µm/s	100kHz	Separated (99.8%)

From the demonstrated results in the last row of Table 6, it can be deduced that the best cell separator should have the following design parameters: 15VPP voltage used among neighboring electrodes at 100 kHz frequency, a flow speed of 150 and 850 µm/s at the upper and lower inlets, respectively. These optimized parameters would improve the device’s separation efficiency, as the resultant separation efficiency of 99.8% was obtained using these modified design parameters.

4. DISCUSSION

In this paper, a modified solution was applied to separate platelets from blood utilizing dielectrophoresis field flow fractionation. The micro-fluid device utilized combining pre-focusing and fractionation functions to specifically trap cells into distinct location relying on their size. The logical cell path was derived from the modeling results demonstrated in this paper. The particle paths were altered by creating a non-uniform electric field and by arranging the electrodes of alternating polarity. Simulations were observed in COMSOL finite element simulation package.

The study simulation results were first verified by comparing it with the original results of the design implemented by Piacentini et al. [25], in which 100 kHz frequency with a voltage of 10VPP was used to separate the PLTs from the RBCs. The experimental results of their study showed a very high separation rate of platelets 98.8% with less cell loss 2%.

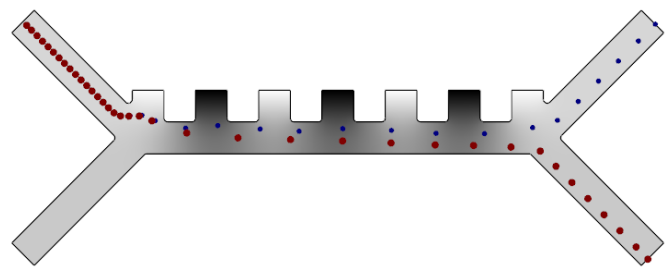


Fig. 5. The voltage applied between electrodes is 15Vpp at 100 kHz, the RBCs are displayed in red and the platelets in blue.

Diverse electric voltages were used to examine the efficiency of electric field on blood sorting (Table IV). The cell paths were computed utilizing the flow velocity used at the upper inlet is 134 µm/s, and the lower inlet is 853 µm/s. The low voltage 5VPP neglected to create adequate FDEP for platelet arranging. Blood cells demonstrate an illustrative flow at the blood inlet. RBCs were not RBCs were not appropriately redirected due to the smaller FDEP. Subsequently, the microfluidic device neglected to separate the diverse blood cells [29]. The form of blood sorting using the electric voltage of 15VPP shows in Fig.5. A suitable FDEP was created to productively sort out the PLTs and RBCs, although the cells were closer to the separator walls, but were still contained within their designated paths. Increasing the electric voltage to 24VPP increased the FDEP on the cell and the electric field. The increase in FDEP made the blood cells divert from the electrodes in the vertical track. Thusly, the PLTs entered the RBCs collection outlet, and the RBCs cell stuck in the device as shown in Fig. 6. These results mean that an electric voltage from 10VPP to 15VPP could be suitable for the proposed model of the microfluidic device to efficiently separate RBCs and PLTs.

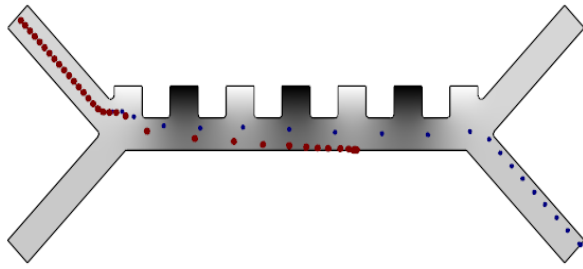


Fig. 6. The voltage applied between electrodes is 24Vpp. The particles followed a similar path, and the RBCs were stuck in the device, the RBCs are displayed in red and the platelets in blue.

The effect of flow speed at the top and the bottom inlets on cell displacement was also examined. The results were processed utilizing 100 kHz frequency at an electric voltage of 10 VPP (Table V). The increased flow speed used at the top and the bottom inlets to reduce the number of blood cells that have been arranged. The higher flow speed utilized at the top and the bottom inlet to increase the movement of the blood cells and the wall collisions region. The separation device is meant to provide an automatic diagnosis tool [30]. In any case, the blood cells that moved with high flow speed used at the top and the bottom inlet were not redirected properly by the FDEP, and subsequently, the number of separated cells was reduced [17,27]. Accordingly, increasing the flow rates essentially reduced the effect of FDEP on the blood cells; and subsequently, the effectiveness of the microfluidic device decreased [31].

5. CONCLUSION

In this paper, a modified solution is applied to separate platelets from blood utilizing dielectrophoresis field flow fractionation. The micro-fluid device utilized adding pre-focusing and fractionation functions to trap cells into distinct places relying on their size specifically. The particle paths were altered by creating a non-uniform electric field and by arranging the electrodes of alternating polarity. The 2D finite element model was exploited to test variations of the design parameters, including the applied separation voltage, frequency, and flow inlet speeds. An electric voltage of 15V is extremely suitable for this modified design to efficiently separate red blood cells and platelets. This modified design can achieve separation with higher efficiency of platelets from RBCs, getting high purity and recovery rates increased by 99.8%. The device's technology makes it especially suitable for bed side point-of-care blood analysis.

6. REFERENCES

- [1] D. F. Stroncek and P. Rebull, "Platelet transfusions," *Lancet*, vol. 370, no. 9585, pp. 427–438, 2007.
- [2] S. J. Slichter and L. A. Harker, "Preparation and Storage of Platelet Concentrates," *Transfusion*, vol. 16, no. 1, pp. 8–12, 1976.
- [3] H. K. Lin et al., "Portable filter-based microdevice for detection and characterization of circulating tumor cells," *Clin. Cancer Res.*, vol. 16, no. 20, pp. 5011–5018, 2010.
- [4] L. Basabe-Desmots et al., "Single-step separation of platelets from whole blood coupled with digital quantification by interfacial platelet cytometry (iPC)," *Langmuir*, vol. 26, no. 18, pp. 14700–14706, 2010.
- [5] A. Lenshof and T. Laurell, "Continuous separation of cells and particles in microfluidic systems," *Chem. Soc. Rev.*, vol. 39, no. 3, p. 1203, 2010.
- [6] G. Dainiak, Maria B. Plieva, Fatima, "Cell Chromatography: Separation of Different Microbial Cells Using IMAC Supermacroporous Monolithic Columns," *Biotechnol. Prog.*, vol. 21, no. 2, pp. 644–649, 2005.
- [7] "Cell Sorting : Automated Separation of Mammalian Cells as a Function of Intracellular Fluorescence Author (s): H . R . Hulett , W . A . Bonner , Janet Barrett and Leonard A . Herzenberg Published by : American Association for the Advancement of Science ," vol. 166, no. 3906, pp. 747–749, 2016.
- [8] P. Yager et al., "Microfluidic diagnostic technologies for global public health," *Nature*, vol. 442, no. 7101, pp. 412–418, 2006.
- [9] W. A. Bonner, H. R. Hulett, R. G. Sweet, and L. A. Herzenberg, "Fluorescence activated cell sorting," *Rev. Sci. Instrum.*, vol. 43, no. 3, pp. 404–409, 1972.
- [10] D. C. Colter, I. Sekiya, and D. J. Prockop, "Identification of a subpopulation of rapidly self-renewing and multipotential adult stem cells in colonies of human marrow stromal cells," *Proc. Natl. Acad. Sci.*, vol. 98, no. 14, pp. 7841–7845, 2001.
- [11] R. David, M. Groebner, and W.-M. Franz, "Magnetic Cell Sorting Purification of Differentiated Embryonic Stem Cells Stably Expressing Truncated Human CD4 as Surface Marker," *Stem Cells*, vol. 23, no. 4, pp. 477–482, 2005.
- [12] E. A. Jones et al., "Isolation and characterization of bone marrow multipotential mesenchymal progenitor cells," *Arthritis Rheum.*, vol. 46, no. 12, pp. 3349–3360, 2002.
- [13] P. Yager, G. J. Domingo, and J. Gerdes, "Point-of-Care Diagnostics for Global Health," *Annu. Rev. Biomed. Eng.*, vol. 10, no. 1, pp. 107–144, 2008.
- [14] B. Weigl, G. Domingo, P. LaBarre, and J. Gerlach, "Towards non- and minimally instrumented, microfluidics-based diagnostic devices," *Lab Chip*, vol. 8, no. 12, p. 1999, 2008.
- [15] C. D. Chin, V. Linder, and S. K. Sia, "Lab-on-a-chip devices for global health: Past studies and future opportunities," *Lab Chip*, vol. 7, no. 1, pp. 41–57, 2007.
- [16] Y. Zhang, S. Park, S. Yang, and T. H. Wang, "An all-in-one microfluidic device for parallel DNA extraction and gene analysis," *Biomed. Microdevices*, vol. 12, no. 6, pp. 1043–1049, 2010.
- [17] Y. Zhang, S. Park, K. Liu, J. Tsuan, S. Yang, and T.-H. Wang, "A surface topography assisted droplet manipulation platform for biomarker detection and pathogen identification," *Lab Chip*, vol. 11, no. 3, pp. 398–406, 2011.
- [18] J. G. E. Gardeniers and A. Van Den Berg, "Lab-on-a-chip systems for biomedical and environmental monitoring," *Anal. Bioanal. Chem.*, vol. 378, no. 7, pp. 1700–1703, 2004.
- [19] S. A. Soper et al., "Point-of-care biosensor systems for cancer diagnostics/prognostics," *Biosens. Bioelectron.*, vol. 21, no. 10, pp. 1932–1942, 2006.
- [20] A. J. Tüdös, G. A. J. Besselink, and R. B. M. Schasfoort, "Trends in miniaturized total analysis systems for point-of-care testing in clinical chemistry," *Lab Chip*, vol. 1, no. 2, pp. 83–95, 2001.
- [21] A. A. H. Sayed, N. Solouma, Y. M. Kadah, "Modeling

- Intrastromal Photorefractive Keratectomy Procedures”, Cairo International Biomedical Engineering Conference, CIBEC, Cairo 2008.
- [22] A. A. H. Sayed, N. Solouma, A. El-Berry, Y. M. Kadah, “Finite Element Models for Computer Simulation of Intrastromal Photorefractive Keratectomy”, *Journal of Mechanics in Medicine and Biology, JMMB*, Vol. 11, 4, 2011.
- [23] M. M. Elramady, A. M. Sayed, M. A. Awadalla, F. S. Mohamed and T. M. Nassef, “Measuring Primary Stability for the Inclined Implants Retaining Mandibular Overdenture using Resonance Frequency”, Cairo International Biomedical Engineering Conference, CIBEC, Cairo 2014.
- [24] M. U. Hamzah, A. M. Sayed and T. M. Nassef, “Computer Assisted Validation of using Newly Introduced Thermoplastic Material in Fabrication of a Telescopic Denture”, *International Journal of Computer Applications, IJCA*, Vol. 181, 15, PP. 16-20, 2018.
- [25] N. Piacentini, G. Mernier, R. Tornay, and P. Renaud, “Separation of platelets from other blood cells in continuous-flow by dielectrophoresis field-flow-fractionation,” *Biomicrofluidics*, vol. 5, no. 3, 2011.
- [26] R. Tornay, T. Braschler, N. Demierre, et al., “Dielectrophoresis-based particle exchanger for the manipulation and surface functionalization of particles,” *Appl. Opt.*, vol. 8, no. 2, pp. 267–273, 2008.
- [27] R. Pethig, “Dielectrophoresis: Status of the theory, technology, and applications,” *Biomicrofluidics*, vol. 4, no. 2, pp. 1–35, 2010.
- [28] B. Sepúlveda et al., “Optical biosensor microsystems based on the integration of highly sensitive Mach–Zehnder interferometer devices,” *J. Opt. A Pure Appl. Opt.*, vol. 8, no. 7, pp. S561–S566, 2006.
- [29] K. Tatsumi, K. Kawano, H. Okui, H. Shintani, and K. Nakabe, “Analysis and measurement of dielectrophoretic manipulation of particles and lymphocytes using rail-type electrodes,” *Med. Eng. Phys.*, vol. 38, no. 1, pp. 24–32, 2016.
- [30] Sayed AM, Zaghoul E, Nassef TM., "Automatic Classification of Breast Tumors Using Features Extracted from Magnetic Resonance Images", *Procedia Computer Science*, Vol. 95, PP. 392-8, 2016.
- [31] Haider Ali, Cheol Woo Park. "Numerical study on the complete blood cell sorting using particle tracing and dielectrophoresis in a microfluidic device", *Korea-Australia Rheology Journal*, 2016